Optical Characterization of Plasma-Polymerized Pyrrole-*N,N*,3,5-Tetramethylaniline Bilayer Thin Films

M. M. Kamal,[1] A. H. Bhuiyan[2]

[1]*School of Engineering and Computer Science, Independent University Bangladesh (IUB), Baridhara, Dhaka 1212, Bangladesh*
[2]*Department of Physics, Bangladesh University of Engineering and Technology (BUET), Ramna, Dhaka 1000, Bangladesh*

Received 2 September 2009; accepted 12 August 2010
DOI 10.1002/app.33176
Published online 21 March 2011 in Wiley Online Library (wileyonlinelibrary.com).

ABSTRACT: A capacitively coupled parallel-plate reactor has been used to deposit plasma-polymerized pyrrole (PPPy), plasma-polymerized *N,N*,3,5-tetramethylaniline (PPTMA), and plasma-polymerized pyrrole-*N,N*,3,5-tetramethylaniline (PPPy-PPTMA) bilayer thin films on to glass substrates at room temperature. To deposit the bilayer films, pyrrole monomer has been used as the mother material and *N,N*,3,5-tetramethylaniline monomer has been deposited in different deposition time ratios after the pyrrole films were formed. Fourier transform infrared (FTIR) and ultraviolet–visible (UV–vis) spectroscopy techniques have been used to characterize the as-grown thin films of about 500-nm thick. The structural analyses by FTIR spectroscopy have indicated that the monomer has undergone the reorganization and the ring structure is retained during the plasma polymerization. From the UV–vis absorption spectra, allowed direct transition (E_{qd}) and allowed indirect transition (E_{qi}) energy gaps were determined. The E_{qd} for PPPy, PPTMA, and PPPy-PPTMA bilayer films are found to be 3.30, 2.85, and 3.65 eV respectively. On the other hand, the E_{qi} for the same series are 2.25, 1.80, and 2.35 eV, respectively. From these results, it is seen that the energy gaps of the PPPy-PPTMA bilayer films have been increased compared with the PPPy and PPTMA films.
 J Appl Polym Sci 121: 2361–2368, 2011

Key words: plasma polymerization; thin films; FTIR; UV–vis spectroscopy; amorphous; energy band gaps

INTRODUCTION

Plasma polymerization is a unique technique to fabricate thin polymer films (100 Å to 1 μm) from a variety of organic and organometallic starting materials. Plasma-polymerized films are usually found to be pinhole-free and highly crosslinked and therefore are insoluble, thermally stable, chemically inert, and mechanically tough. Furthermore, such films are often highly coherent and adherent to a variety of substrates including conventional polymer, glass, and metal surfaces. Because of these excellent properties, they have been undertaken very actively in the last few years for a variety of applications such as protective coatings, membranes, biomedical materials, electronic and optical devices, adhesion promoters, anticorrosive surfaces, humidity sensors, electrical resistors, scratch resistant coatings, optical filters, protective coatings, chemical barrier coatings, etc. The generation of multilayer/composite materials also has a wide variety of applications, e.g., in biocompatible materials, in the modification of surfaces, in protective coverings of metals, in the design of complex materials, etc.[1] Plasma polymerization is a versatile technique for the deposition of thin films with functional properties suitable for a wide range of modern applications, because the molecular structures of the films are different from starting materials, since they are formed with fragmented molecules under ions and electron collisions with high energy.[2,3]

Various properties of the polymers such as structural, physical, chemical, optical, and electrical properties have been investigated as appeared in literatures. Yasuda et al.[4] and Westwood[5] investigated the elemental compositions of plasma polymers produced from a variety of organic compounds using various kinds of plasma reactors. They observed two trends in the plasma polymers namely: (i) the deficiency of hydrogen and halogens that are attached to the carbon in the monomers and (ii) the incorporation of oxygen in the polymers even though the monomers do not contain oxygen. Having these observations, they concluded that the incorporation of oxygen is a consequence of the post plasma reaction of trapped free radicals with ambient oxygen. Jesch et al.[6] studied the Fourier transform infrared

Correspondence to: M. M. Kamal (mkamal@secs.iub.edu.bd).

Contract grant sponsors: Bangladesh University of Engineering and Technology (BUET), Dhaka, Independent University, Bangladesh.

(FTIR) spectra of plasma polymers formed from pentane, ethylene, butadiene, benzene, styrene, and naphthalene. On the basis of the structures analyzed by FTIR spectroscopy, they concluded that whether the monomer was aromatic or olefinic or fully saturated, the plasma polymer was highly branched and crosslinked and contains identifiable saturation. Different properties of plasma polymerized and iodine-doped polypyrrole have been investigated by Rajan et al.[7] A comparative study of the FTIR spectra of the monomer and polymer pyrrole gives information that the ring structure is retained during plasma polymerization. Valaski et al.,[8] Eufinger et al.,[9] Kumar et al.[10] also did the detail study on the characterization of polymerized pyrrole thin films. Bhuiyan et al.[11] calculated the optical band gaps of plasma-polymerized acrylonitrilc thin films from absorption edge maxima and found that the band gap was modified on doping in contrast to the behavior of inorganic semiconductors, where band gap remains unaffected on doping. Xiao et al.[12] investigated on the preparation, characteristics, and different properties of plasma polymerized nitriles. In their study, FTIR, UV–vis, X-ray photoelectron spectroscopy (XPS), atomic force microcopy (AFM), and deposition rate characterization revealed that the plasma synthesis conditions affected the chemical structure, surface composition, morphology, and property of the plasma deposited films. Akther and Bhuiyan[13] did the FTIR and UV–vis spectroscopic investigation of plasma-polymerized *N,N*,3,5-tetramethylaniline (PPTMA) thin films. The structural analysis revealed that PPTMA thin films are formed with certain amount of conjugation that modifies on heat treatment. From the UV–vis absorption spectra, allowed direct transition (E_{qd}) and indirect transition (E_{qi}) energy gap are determined and it is seen that while E_{qd} increases a little, E_{qi} decreases, on heat treatment of PPTMA. The calculated value of Tauc parameter B for the entire sample indicates an increase in structural order/conjugation in PPTMA thin films on heat treatment. It is then concluded that PPTMA thin film with conjugation can be produced by plasma polymerization and the structural order can be improved by heat treatment. The allowed direct and indirect transition energy gaps are also modified when the samples are heat treated.

The electronic conductivity of bilayer aniline (PAn)-pyrrole (Py) thin films have been studied by Morales et al.[1,14] The obtained results indicated that the plasma technique was capable of forming chemically bonded layered polymers with several possible combinations. They found that the synthesis of the iodine-doped bilayer PAn-polymerized pyrrole (PPy) polymers by plasma allows to controlling the thickness of each layer, creating the possibility of having thin films of different materials chemically bonded at the interface by a complex mechanism of layers that join and separate in several areas. With this technique, the studied polymers can be doped with greater percentages of iodine, so that the polymers have better electrical properties. Another characteristic is that the films with PAn have lower thermal stability because PAn tends to release the iodine atoms at a lower temperature than the PPy chains. Finally they found that, the bilayer PAn-Py polymers had greater electric conductivity at room temperature than that shown by the separate homopolymers. Organic films were prepared by RF plasma chemical vapor deposition (CVD) using naphthalene (named naph), propane (prop), and naphthalene-mixed propane (naph-prop) by Tengku Nadzlin et al.[15] From their study on the optical and electrical properties of the films, they found that all of the samples showed broadband emission of photoluminescence. The aromatic and aliphatic rings found in FTIR transmission for all samples showed that the samples contained the original monomer. The conductivity of the samples showed that mixed film (naph-prop sample) performed larger current flow than the single monomer film (naph and prop samples) and showed SCLC behavior for the conduction mechanism at the higher voltage region. Plasma-deposited polymer films were prepared by Swaraj et al.[16] from organic molecules. Aging effects of plasma-deposited organic films after exposure to air were investigated using near-edge X-ray absorption fine structure (NEXAFS) and XPS in terms of changes in the oxygen or nitrogen concentration, changes in the content of unsaturated or aromatic species, and changes in the concentration of monomer functionality. In general, change in content of unsaturated or aromatic species, change in concentration of monomer functionality, and change in the oxygen content was observed in the plasma polymerized films on aging. The electrical and optical properties of natural and synthetic melanin were characterized using optical, electrical, and photo electronic measurements by Ligonzo et al.[17] The optical gap for synthetic melanin were estimated by using Tauc's method from absorption curves and found to be 1.39 eV, while it was not possible to evaluate for natural melanin due to an exponential behavior of absorption spectrum. Dark conductivity and photo conductivity were characterized as a function of temperature and for different duration of thermal treatments and it is found that both quantities are thermally activated and thermal treatments play an important role as far as gap states are concerned. It is also seen that the dark conductivity increases after thermal treatments and also photoconductivity improves especially in the UV spectral range.

This article describes the preparation of plasma-polymerized pyrrole-PPTMA (PPPy-PPTMA) bilayer

thin films by plasma polymerization and discusses the chemical structure investigated by FTIR spectroscopy and optical properties of the thin films studied by UV–vis spectroscopy. It is to be noted that derivatives of PAn and Py are very well-known organic materials. Different properties of plasma-polymerized thin film of these organic materials have been reported by many investigators. These two materials are chosen to prepare and characterize the bilayer thin film, because it is usually observed that the bilayer and composite thin films give rise to different properties than the films prepared with single monomers. The results that are obtained for PPPy-PPTMA bilayer thin films are compared with those of the thin films prepared from component monomers, i.e., PPPy and PPTMA thin films.

EXPERIMENTAL

Sample preparation

A capacitively coupled parallel-plate reactor has been used to deposit PPPy, PPTMA, and PPPy-PPTMA bilayer thin films on to glass substrates at room temperature. To deposit the bilayer films, pyrrole monomer has been used as the mother material and TMA monomer has been deposited in different deposition time ratio after the pyrrole films were formed.

The monomers pyrrole and the TMA were collected from Aldrich-Chemie D-7924, Steinheim, Germany. The monomer vapors were introduced to the reactor through a flowmeter at the flow rate of about 20 cm^3 (STP)/min into the glow discharge reactor. The glow discharge system is a bell jar-type capacitively coupled system and consists of two parallel plate electrodes of stainless steel of diameter and thickness 0.09 and 0.001 m, respectively, and placed 0.035 m apart. The glow discharge chamber was evacuated by a rotary pump (Vacuubrand, Vacuubrand GMBH and Co, 97877 Wertheim, Germany) and plasma was generated around the substrates, which were kept on the lower electrode, using a step-up transformer connected to the electrodes with a power of about 30 W at line frequency. Transparent light yellow-colored PPPy, PPTMA, and PPPy-PTMA bilayer thin films of different thickness were deposited onto the glass substrates. The deposition parameters such as flow-rate, deposition-time, power, and vacuum order were kept almost same for all samples so that the comparison of the results could be made for various plasma polymerized samples. The thicknesses of deposited films were measured by a multiple-beam interferometric technique.

Fourier transform infrared (FTIR) spectroscopy

For FTIR studies, the as-grown PPPy, PPTMA, and PPPy-PPTMA bilayer thin film were scraped off from the glass substrates in powder form and were mixed with potassium bromide (KBr). This mixture was then pelletized. These pellets of the mixture were used to record the FTIR spectra at room temperature using an FTIR spectrometer (Shimadzu -IR 470, Shimadzu Corp., Tokyo, Japan). All the spectra were recorded in transmittance (%) mode in the wavenumber region 4000–500 cm^{-1}.

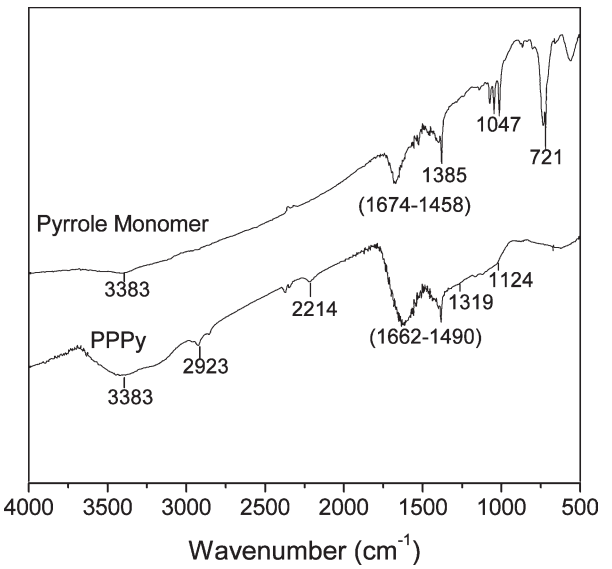

Figure 1 The FTIR spectra of pyrrole monomer and PPPy.

UV–vis spectroscopy

UV–vis spectra of as grown PPPy, PPTMA, and PPPy-PPTMA thin films on glass substrates were obtained in absorption mode with a spectrophotometer Shimadzu UV-160A (Shimadzu Corp., Tokyo, Japan) in the wavelength range 200–800 nm at room temperature.

RESULTS AND DISCUSSION

FTIR spectroscopic analyses

Figure 1 represents the FTIR spectra of pyrrole monomer and PPPy, and in Table I, the peak assignments for the pyrrole monomer and peak assignments for the PPPy thin films are shown. In the FTIR spectrum of the monomer of pyrrole and PPPy (Fig. 1), the absorption bands are found to be very close to those reported previously.[7,9,10] It is seen that the FTIR spectrum of the PPPy is relatively complicated than that of the pyrrole monomer. Both spectra show a strong peak at about 3383 cm^{-1}, which is due to the N—H bond stretching vibration of primary and secondary amines and imines.[9] The absorption around 1650 cm^{-1} corresponds to the amines in the pyrrole structure. At about 2923 cm^{-1},

TABLE I
Assignments of FTIR Absorption Peaks for Pyrrole, PPPy, TMA, PPTMA, and PPPy-PPTMA Bilayer Films

Vibrations	Wavenumber (cm^{-1})				
	Pyrrole	PPPy	TMA	PPTMA	PPPy-PPTMA
N—H stretching vibration of primary and secondary amines	3383	3383	3475	3435	3385
Symmetric N—H stretching vibration	–	–	3340	–	–
Asymmetric and symmetric C—H stretching vibration of saturated hydrocarbon	–	2923	2935, 2793	2935	2924
—N=C=O	–	2214	–	–	2214
C=O	–	–	–	1850-1603	–
C=C conjugated and C=N conjugated stretch and N—H deformation vibration	1674–1458	1652–1490	–	–	1652-1458
C=C stretching vibration	–	–	1680-1645		–
C=C stretching vib. in benzenoid and quinoid	–	–	1595, 1484	1570, 1472	1610, 1508
Alkane C—H deformation	1384	–	–	–	1384
C—N stretching vibration	1047	1124	1351, 1307, 1223–1030	1340	1128
Tetrasubstituted benzene	–	–	814 - 776	–	–
C—H out of plane bending	721	–	–	–	–

there is a sharp peak in PPPy spectrum but not in monomer spectrum. The peak is due to asymmetric and symmetric C—H stretching vibration of saturated hydrocarbon. Pyrrole has highly strained ring so that the ring is easy to open under plasma polymerization. Therefore, the FTIR spectrum of PPPy is very different to that of the monomer. In the molecular structure of the pyrrole monomer, all the carbon atoms are unsaturated. Thus, the peaks around 2900 cm^{-1} come from the plasma polymerization. There is another special peak around 720 cm^{-1} appearing in the spectrum of pyrrole monomer, but not in the spectrum of PPPy. This peak usually belongs to $—CH_2—$ unites. All of these differences indicated that the monomer undergone the reorganization during the plasma polymerization.

Figure 2 shows the FTIR spectra of TMA and PPTMA and in Table I the peak assignments for TMA and PPTMA are presented. In this spectrum, the absorption bands at around 3435, 2935, 1850–1603, 1570, 1472, and 1340 cm^{-1} in the wide absorption envelope resulting from the presence of N—H stretching vibration, C—H stretching vibration, an aromatic ring C=C stretching vibration in benzenoid and quinoid rings and CN stretching vibration, respectively.[13] The wide band around 1850–1603 cm^{-1} may also include the contribution due to C=O stretching vibration that is typical for plasma polymers. The formation of carbonyl group is usually attributed to the oxidation of the hydrocarbon part of the PPTMA after exposure to air owing to oxygen reactions with a radical species (dangling bonds) trapped in the structure of the plasma polymer. Crosslinking may also occur between different carbons of the chains due to the loss of hydrogen, particularly in the plasma-polymerized films because of the impact of energetic particles within the plasma during deposition. Here the PPTMA shows a widening of the band corresponding to the C=C stretching vibration of benzenoid and quinoid and slight downshifting of CN stretching vibrations, probably caused by crosslinking interactions intrinsically associated with plasma polymers. The FTIR observations reveal that the PPTMA contain an aromatic ring structure with NC and CH side groups. From the above discussion, it is understood that the PPTMA film deposited by the plasma polymerization technique does not exactly resemble to that of the TMA structure.

Figure 3 represents the FTIR spectra of the PPPy-PPTMA bilayer thin films and in Table I the peak

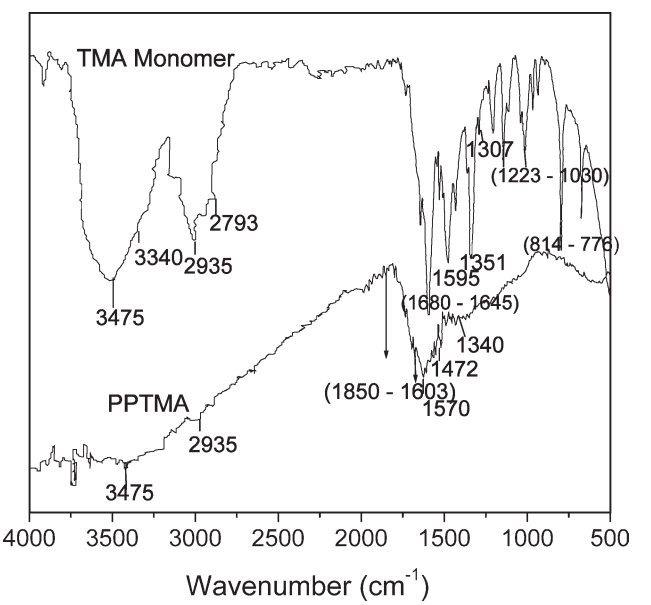

Figure 2 The FTIR spectra of TMA monomer and PPTMA.

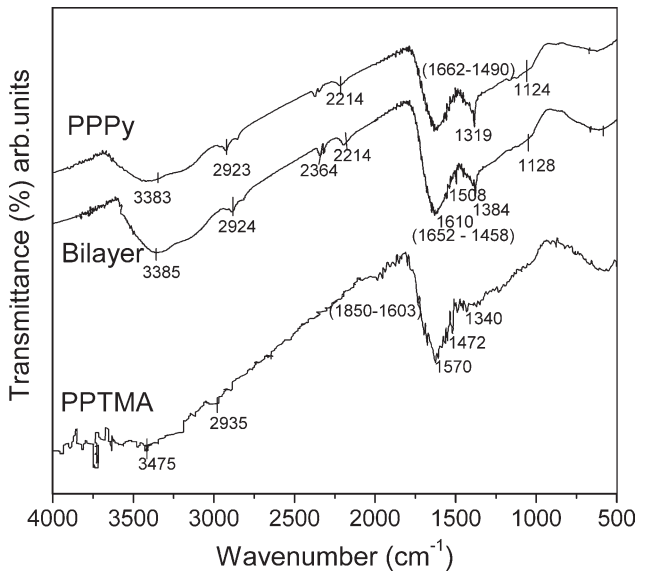

Figure 3 The FTIR spectra of PPPy, PPTMA, and PPPy-PPTMA bilayer thin film.

assignments for the Figure 3 is also given. For comparative study, the FTIR spectra of PPPy and PPTMA thin films are also presented in this figure.

Comparison to FTIR spectra of PPPy and PPPy-PPTMA bilayer films, it is seen that both the spectra exhibit a broad band between 3300 and 3400 cm^{-1}, which is due to the N—H stretching vibration of primary and secondary amines and imines.[9] In the bilayer film, the relative intensity of this peak is higher than that in the PPPy film. The bilayer film has a relatively more intense peak at 2924 cm^{-1} compared with 2923 cm^{-1} of PPPy film and 2935 cm^{-1} of PPTMA films, which is due to the symmetric and asymmetric C—H stretching vibration of saturated hydrocarbons. As the peak around 2930 cm^{-1} can be attributed to the asymmetric CH_2 vibration, it can be suggested that the bilayer film contains more methylene groups than the other films. In addition to this, the bilayer spectrum exhibits peak at 1384 cm^{-1} which is due to the C—H deformation of a CH_3 group. This again shows that the bilayer film contains more methylene groups than the PPPy or PPTMA films. The absorption peak at 2214 cm^{-1} in both PPPy and PPPy-PPTMA films suggests the introduction of —N=C=O group,[18,19] which is very typical in plasma polymerization.[4,5] The absorption at 1508 and 1610 cm^{-1} of bilayer films can be assigned to the benzoid and quinoid structures of the benzene rings in TMA. As expected, they are found due to the presence of TMA, because pyrrole does not contain any benzene rings. This study, however, shows that the bilayer films contain the characteristics of both the monomer.

UV–vis spectroscopy

The UV–vis absorption spectra of as deposited PPPy, PPTMA, and PPPy-PPTMA thin films have been recorded at room temperature. In Figure 4, a comparative study on the variation of absorption (ABS) with wavelength, λ, for as deposited PPPy, PPTMA, and PPPy-PPTMA bilayer films of nearly equal thickness (500 ± 10) nm are presented. It is to be noted that this sample of PPPy-PPTMA bilayer thin film has been formed by depositing pyrrole monomer for 40 min and then TMA monomers for 20 min. It is, however, observed in the UV–vis spectra of Figure 4 that, the peak wavelength value, λ_{max}, for PPPy, PPTMA, and bilayer thin films are 300 nm, 380 nm and 300 nm, respectively, i.e., the peak of PPPy and bilayer thin films are formed at the same λ_{max} value. However, the intensity of the absorption (peak) of the bilayer film reduced to almost half of the value that of the PPPy films, but reached to very close to the intensity of the absorption of PPTMA.

The absorption coefficient, also called the optical density, α was calculated from the absorbance data of Figure 4 using the relation[20]:

$$\alpha = 2.303(A/d) \quad (1)$$

where A is the absorbance and d is the thickness of the thin film.

The spectral dependence of α as a function of energy $h\nu$ is shown in Figure 5. It is observed that in the low energy region the edges follow linear fall for values of α below about 5000 cm^{-1} for all types of samples. These falling edges may either be due to

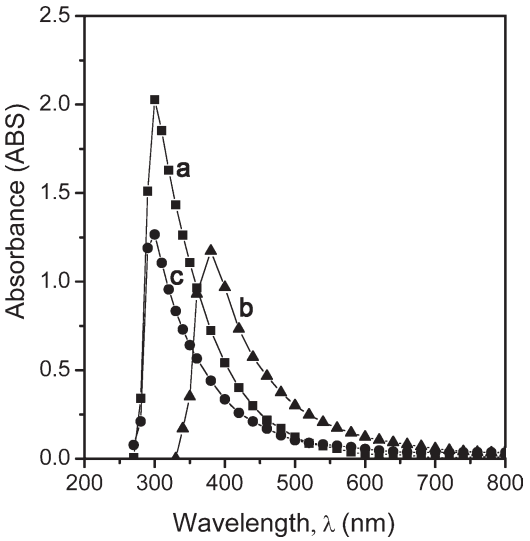

Figure 4 Variation of absorption (ABS) with wavelength, λ, for as grown (a) PPPy, (b) PPTMA, and (c) PPPy-PPTMA bilayer thin films.

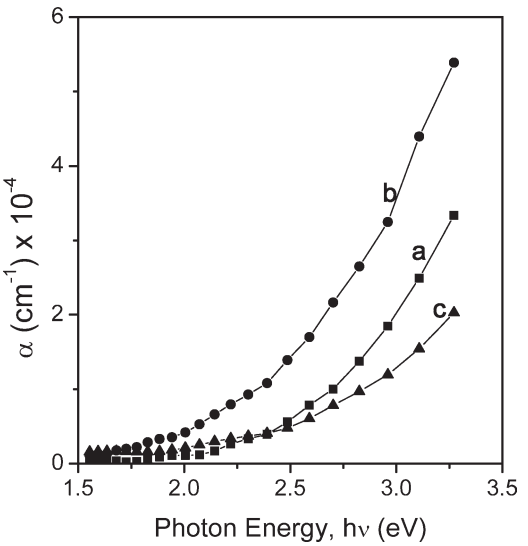

Figure 5 Plots of absorption coefficient, α, as a function of photon energy, $h\nu$, for as grown (a) PPPy, (b) PPTMA, and (c) PPPy-PPTMA bilayer thin films

lack of long-range order or due to the presence of defects in the thin films.[21]

The extinction coefficient, K, can be computed from the optical density α, by using the relation:

$$\alpha = \frac{4\pi K}{\lambda} \tag{2}$$

where λ is the wavelength. The variation of K (or variation of α) of thin films with the photon energy, $h\nu$, has an important meaning. The increase of K with the increase of $h\nu$ indicates the probability of raising the electron transfers across the mobility gap with the photon energy. As the bilayer thin film has less optical density while its components show a higher extinction, therefore the probabilities of electron transfers across the mobility gap are higher for PPPy and PPTMA thin films than that of the bilayer films.

It could be noted that the absorption coefficient α has been calculated from the experimental absorption data of the PPPy-PPTMA bilayer thin film and found to be reduced than that of both the component thin films, i.e., PPPy and PPTMA. The α, however, could also be calculated for an ideal bilayer thin films from the absorption data of the component films, by using the following equation:

$$\alpha' = \frac{\alpha_1 d_1 + \alpha_2 d_2}{d_1 + d_2} \tag{3}$$

where α_i and d_i are the absorption coefficient and thickness of the components respectively, and α′ is the absorption coefficient of the PPPy-PPTMA ideal bilayer thin films which has been calculated from the absorption data of the individual components by using the Eq. (3). It should be noted that the relationship between components thickness has been evaluated from Figure 4 with an approximation of PPPy : PPTMA = 0.6 : 0.4, with $d = 1$ as the bilayer thickness, as the bilayer film of Figure 4 was prepared by depositing the PPPy and PPTMA thin films with a deposition time ratio (40 + 20 min). The theoretically calculated values of α′ for the ideal bilayer thin films from the absorption data of the individual components has been plotted in Figure 6 as a function of photon energy, $h\nu$, to compare with the α calculated from experimental absorption data of real PPPy-PPTMA bilayer thin films. The α′s for component thin films (PPPy and PPTMA) are also shown in the same figure for comparison.

It is seen from the Figure 6 that the theoretically calculated values of the absorption coefficient α′ lie in between the values of α of the two individual components; whereas the experimental values of α indicate an apparent reduction in absorption coefficient of the bilayer films with respect to that of its components. The difference in Urbach tails of the real and ideal bilayer thin films indicates different activation energy in the real bilayer film (curve c) than what would be expected from the ideal situation (curve d). Like any other ideal bilayer of two materials without interface effect, where the physical properties of the bilayer usually lie in between of those of the original materials, in the present case the ideal PPPy-PPTMA bilayer films shows a similar behavior. As both PPPy and PPTMA layers

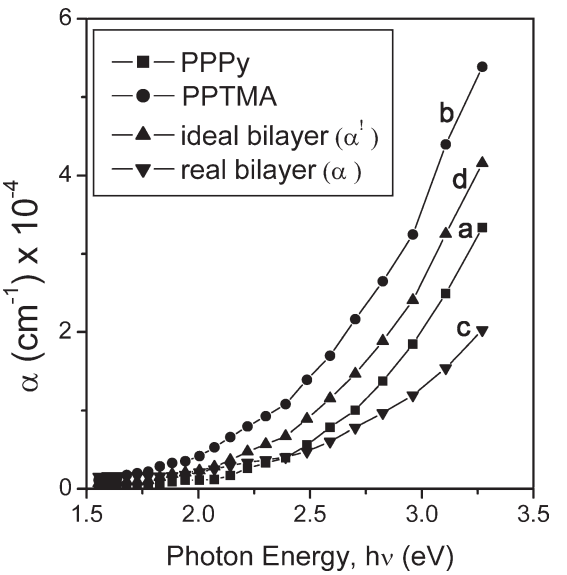

Figure 6 Plots of absorption coefficient, α, as a function of photon energy, $h\nu$, for as grown (a) PPPy, (b) PPTMA, (c) PPPy-PPTMA real bilayer thin films, and (d) PPPy-PPTMA ideal bilayer thin films.

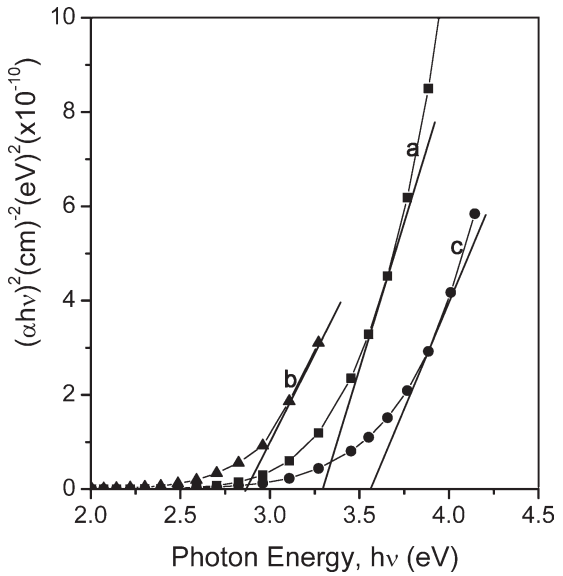

Figure 7 $(\alpha h\nu)^2$ versus $h\nu$ curves of (a) PPPy, (b) PPTMA, (c) PPPy-PPTMA bilayer thin films.

in the bilayer thin film have the same structure as in the component films, therefore the result, that the theoretical values of absorption coefficient α' of the PPPy-PPTMA ideal bilayer films lies in between those of the components, is not unexpected. However, when the absorption coefficient is calculated from the absorption data of the components, the interaction in the interface of the two component thin films could not be considered. In our study, as thin films of the components were deposited one over the other to prepare the PPPy-PPTMA bilayer thin films by using plasma polymerization technique, therefore the interaction in the interface has occurred which may give rise to a system with polymer–polymer complex interface between the PPPy and PPTMA thin films. This complex interface may not be homogeneous and therefore, there are some possibilities of presence of irregularities in the interface which may cause more amorphous structure of the bilayer thin film. It should be noted that in most inhomogeneous/amorphous polymeric systems, the electronic conductivity is affected by this interface. The cross-linking between the interfaces should also be taken into consideration in this system, which may cause less absorption coefficient and consequently higher optical band gaps.

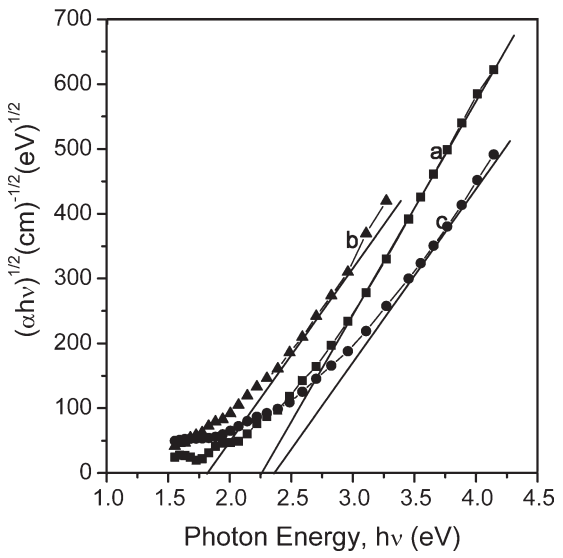

Figure 8 $(\alpha h\nu)^{1/2}$ versus $h\nu$ curves of (a) PPPy, (b) PPTMA, (c) PPPy-PPTMA bilayer thin films.

One of the most significant optical parameters, which is related to the electronic structure, is the optical band gap. The optical band gap, E_{opt}, can be calculated by Tauc relation[22]

$$\alpha h\nu = B(E_{opt} - h\nu)^n \quad (4)$$

where B is the Tauc parameter, n is the parameter connected with distribution of the density of states, and E_{opt} is the optical band gap obtained from the extrapolation of the linear part of the curve.

To indicate the presence of direct and indirect transitions in the materials, the curves in Figure 5 could be characterized by two different slopes. The allowed direct transition energy gap can be evaluated from the plots of $(\alpha h\nu)^2$ as a function of $h\nu$ shown in Figure 7. The allowed indirect transition energy gap can be evaluated from $(\alpha h\nu)^{1/2}$ versus $h\nu$ plots in Figure 8. Both the energy gaps are determined from the intercept of the extrapolation of the curves to zero α in the photon energy axis. The values of allowed direct transition energy gap, E_{qd}, and allowed indirect transition energy gap, E_{qi}, obtained from the plots of Figure 7 and Figure 8 are documented in Table II.

From Table II it is seen that the energy gaps of the PPPy-PPTMA bilayer films are increased compared with those of the PPPy and PPTMA films.

TABLE II
Allowed Direct and Allowed Indirect Transition Energy Gaps for PPPy, PPTMA, and PPPy-PPTMA Bilayer Thin Films

Samples	Direct transition energy gap, E_{qd} (eV)	Indirect transition energy gap, E_{qi} (eV)
PPPy	3.30	2.25
PPTMA	2.85	1.80
PPPy-PPTMA bilayer	3.65	2.35

The incorporation of oxygen in plasma polymer as a contamination may be due to the reaction of trapped free radicals with oxygen from the plasma reactor even though the monomers do not contain oxygen.[4] The FTIR analyses of PPPy, PPTMA, and PPPy-PPTMA films in this study have also indicated the presence of oxygen by the appearance of the absorption band at 2214, 1850–1603, and 2214 cm^{-1}, respectively, Therefore, during the subsequent formation of the films by plasma polymerization, there may be adsorbed and/or trapped oxygen of the interface in between the PPPy and PPTMA thin film layers. The oxidation of the interface of the bilayer might affect the physical properties of the bilayer thin films. The increase of optical band gap may be due to this reason. Furthermore, it is observed that the electrical resistivity of the PPPy-PPTMA bilayer thin films is higher than those of the individual component thin films, which has been addressed in a separate communication.

CONCLUSIONS

The PPPy, PPTMA, and PPPy-PPTMA bilayer thin films were prepared using a capacitively coupled parallel plate reactor. It is observed from FTIR analyses that the pyrrole undergone reorganization in its chemical structure during the plasma polymerization. This technique yields PPTMA thin films with conjugation. The study, however, shows that the PPPy-PPTMA bilayer films contain, more or less, the characteristics of both the monomer.

The energy gaps E_{qd} and E_{qi} were calculated from UV–vis spectroscopic investigation and are found to be 3.30 eV and 2.25 eV for as grown PPPy, 2.85 eV and 1.80 eV for PPTMA and 3.65 eV and 2.35 eV for PPPy-PPTMA bilayer thin films. It is seen that, both the E_{qd} and the E_{qi}, are higher for PPPy-PPTMA bilayer films than the PPPy and PPTMA. The higher value of the optical band gap of the bilayer films might result owing to the oxidation at the interface of the PPPy-PPTMA bilayer during subsequent deposition of the bilayer thin films.

The authors would like to acknowledge the help of BCSIR for providing the laboratory facilities to record the UV–vis and the FTIR spectra.

References

1. Morales, J.; Olayo, M. G.; Cruz, G. J.; Olayo, R. J Polym Sci Part B: Polym Phys 2002, 40, 1850.
2. Chowdhury, F.-U.-Z.; Bhuiyan, A. H. Thin Solid Films 2000, 306, 69.
3. Quan, Y. C.; Yeo, S.; Shim, C.; Yang, J.; Jung, D. J Appl Phys 2001, 89, 1402.
4. Yasuda, H.; Bumgarner, M. O.; Marsh, H. C.; Morosoff, N. J Polym Sci Polym Chem Ed 1976, 14, 195.
5. Westwood, A. R. Eur Polym Mater 1971, 7, 377.
6. Jesch, J.; Bloor, J. E.; Kronick, P. C. J Polym Sci 1966, 14, 1487.
7. John Rajan, K.; Shakti Kumar, D. J Appl Polym Sci 2002, 83, 1856.
8. Valaski, R.; Ayoub, S.; Micaroni, L.; Hümmelgen, I. A. Thin Solid Films 2002, 415, 206.
9. Eufinger, S.; Van Ooij, W. J.; Ridgway, H. J Appl Polym Sci 1966, 61, 1503.
10. Sakthi Kumar, D.; Nakamura, K.; Nishiyama, S.; Ishii, S.; Noguchi, H.; Kashiwagi, K.; Yoshida, Y. J Appl Phys 2003, 93, 2705.
11. Bhuiyan, A. H.; Rajopadhye, N. R.; Bhoraskar, S. V. Thin Solid Films 1988, 161, 187.
12. Xiao, H.; Xiongyan, Z.; Uddin, A.; Lee, C. B. Thin Solid Films 2005, 477, 81.
13. Akther, H.; Bhuiyan, A. H. Thin Solid Films 2005, 474, 14.
14. Morales, J; Olayo, M. G.; Cruz, G. J.; Castillo-Ortega, M. M.; Olayo, R. J Appl Polym Sci 2000, 38, 3247.
15. Tengku Ibrahim, T. N. B; Tanaka, K.; Uchiki, H. Jpn J Appl Phys 2008, 47, 794.
16. Swaraj, S.; Oran, U.; Lippitz, A.; Friedrich, J. F.; Unger, W. E. S. Plasma Process Polym 2007, 4, 784.
17. Ligonzo, T.; Ambrico, M.; Augelli, V.; Perna, G.; Schiavulli, L.; Tamma, M. A.; Biagi, P. F.; Minafra, A.; Capozzi, V. J Non-Crystalline Solids 2009, 355, 1221.
18. Zhang, J.; Wu, M. Z.; Pu, T. S.; Zhang, Z. Y.; Jin, R. P.; Tong, Z. S.; Zhu, D. Z.; Cao, D. X.; Zhu, F. Y.; Cao, J. Q. Thin Solid Films 1997, 307, 14.
19. Fally, F.; Doneux, C.; Riga, J.; Verbist, J. J. J Appl Polym Sci 1995, 56, 597.
20. Al-Ani, S. K. J.; Higazy, A. A. J Mater Sci 1991, 26, 3670.
21. Davis, E. A.; Mott, N. F. Phil Mag 1970, 22, 903.
22. Tauc, J. In Amorphous and Liquid Semiconductors; Tauc, J. Ed; Plenum: London, 1974; Chapter 4.